Materials Transactions, Vol. 43, No. 5 (2002) pp. 1037 to 1044
Special Issue on Smart Materials-Fundamentals and Applications

Shape-Memory Micropumps

Yi-Chung Shu *

Institute of Applied Mechanics, National Taiwan University, Taipei 106, Taiwan, R.O. China

Motivated by many experimental efforts to develop suitable shape-memory micropumps, we propose a multiscale framework to study the behavior of pressurized films. We use recoverable deflection as a measure to design large stroke micropumps and develop a model to estimate it. We show that the recoverable deflection of a polycrystalline shape-memory film depends on the transformation strain of the underlying martensitic transformation, the texture and especially on the size effects. We find that flat grains are preferable to long grains in columnar films concerning the purpose of large recoverable strain. We also show that common sputtering texture is not ideal for recoverable deflection in both Ti–Ni and Cu-based shape-memory films. It turns out that {100} Cu-based films may have better behavior than Ti–Ni films. We conclude with comparison with experiment.

(Received November 19, 2001; Accepted February 27, 2002)

Keywords: *pressurized shape-memory films, recoverable deflection, size effect*

1. Introduction

The interest in microelectromechanical system (MEMS) applications has recently motivated many experimental efforts to develop suitable microactuators and micropumps. These devices have a wide range of applications in fields such as drug delivery, inkjet printing and cooling systems of electronic circuits. However, common MEMS-integrated actuation scheme has enjoyed limited success in delivering a reasonable work output from the extremely small size of devices, and therefore both high stroke and force are the key requirement for selecting actuating materials. Shape-memory alloys show great promise in this aspect since their work density is significantly higher than that of other types of materials.[26) These alloys are able to recover large strain and are capable of high force, which in turn directly transmit large stoke and high pressure in micropumps. In addition, the disadvantage of low response rate caused by cooling and heating bulk shape-memory alloys can be greatly improved at small scales because of the increase in the surface area to volume ratio. This makes these alloys in the form of thin films ideal for use in MEMS-integrated actuation scheme, and we seek to develop a micromechanical model to understand the behavior of film at an extremely small thickness.

In this paper, we propose a framework to study the behavior of pressurized shape-memory thin films with intended application to large stoke micropumps. Our work was motivated by the recent experiment on the fabrication of SMA actuated micropumps.[16,17,26)] They have reported that a Ti–Ni micropump exhibits the largest work out per cycle per unit volume amongst various common actuator systems.[26)] However, the ratio of the deflection to the half-edge length of diaphragm has been observed around several values from 0.04 to 0.12 which only correspond to 0.2%–1.4% small strain. Our theoretical prediction is around 0.15 which is larger than these experimental observations, and the discrepancy is not completely understood here. We believe there should be a plenty of room to improve this critical ratio to design large stroke micropumps. In particular, we show that {100} Cu-based shape-memory thin films may have better behavior than Ti–Ni films in view of large recoverable deflection.

We present the general framework of pressurized films following Shu[21,22)] in Sec. 2. We consider a film released from the substrate in some chosen region, but attached to it outside as shown in Fig. 1. The film considered here consists of multiple layers, each of which contains many grains. The layered material can be martensitic. Therefore, there are three length scales: the film thickness, grain size and microstructure length scale as seen in Fig. 1. We assume that all these length scales are much smaller than the lateral extent of the film. Depending on the deposition technique, the size of grains within the film can be larger than, comparable to or smaller than the thickness of film. Furthermore, depending on the material, the length scale of microstructure can also be larger than, comparable to or smaller than that of grains. Thus, the behavior of the heterogeneous film shows strong size effects, and we seek to understand it by introducing the *effective theory*. We use the framework of Γ-convergence to show that the limiting behavior of the film is determined by an effective two-dimensional theory which depends crucially on ratios between these three length scales. We use the effective theory and the Taylor bound to estimate recoverable strain in Sec. 3. We study the effect of texture and grain size on recoverable strain in Sec. 4. We show that flat grains are preferable to long grains in columnar films and find that sputtering textures in both Ti–Ni and Cu-based films are not favorable for large recoverable strain. We also use our theory to explore multilayered films and the novel properties that they may possess.

We apply our results to the design of large stroke shape-memory micropumps in Sec. 5. The stroke of a micropump determines the volume pumped per cycle, and therefore we use the ratio of central deflection to the half-edge length of the diaphragm as our design criterion. We use the assumption of von Kármán membrane to approximate the finite strain measure to estimate deflection of the symmetric diaphragm. We demonstrate with an example that the result obtained using simplified kinematics agrees very well with that estimated using the fully nonlinear kinematics developed by Bhattacharya

*E-mail: yichung@spring.iam.ntu.edu.tw

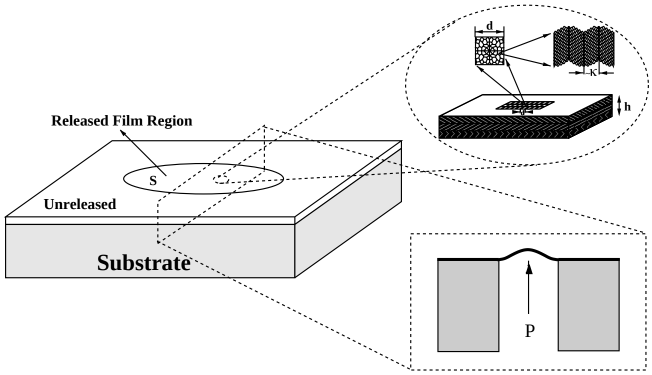

Fig. 1 Prototype of a micropump using shape-memory material. The film is heterogeneous and contains three different length scales h, d and κ. It is released from the substrate in the chosen region S, but attached to it outside.

& James.[3,10] We then extend the analysis to estimate recoverable deflection for polycrystalline shape-memory films. We consider columnar films with grain size much larger than film thickness. Table 2 lists our main prediction for recoverable deflection for various films with different textures. It shows that recoverable deflection is not sensitive to common film textures in Ti–Ni films while it is sensitive in Cu-based shape-memory films. It turns out that {100} texture is ideal for both recoverable deflection and extension in Cu-based films. We compare our prediction with experiment in Sec. 6 and conclude in Sec. 7 with a discussion.

2. Theory

Consider a heterogeneous (possibly multilayered) thin film released from the substrate in a well-defined region S, but constrained on its lateral boundaries as shown in Fig. 1. Since we anticipate large strain for shape-memory materials, we use the setting of finite deformations. Let $\boldsymbol{x} = (x_1, x_2, x_3)$ be the material point of the film relative to an orthonormal basis $\{\boldsymbol{e}_1, \boldsymbol{e}_2, \boldsymbol{e}_3\}$. The deformation of the film is denoted by $\boldsymbol{y} = (y_1, y_2, y_3)$ which is the function of the material point $\boldsymbol{x}$. Let h be the film thickness and d be the period of the in-plane texture (in other words, d is the typical length scale of the representative area element in the film plane). Let the in-plane variables x_1 and x_2 be normalized by d and the out-of-plane variable x_3 by h. Thus, the elastic energy density of this heterogeneous film is

$$\varphi = \varphi\left(\boldsymbol{F},\ \frac{x_1}{d},\ \frac{x_2}{d},\ \frac{x_3}{h}\right),$$
$$F_{ij}(\boldsymbol{x}) = \frac{\partial y_i(\boldsymbol{x})}{\partial x_j} \quad \text{for} \quad i,\ j = 1,\ 2,\ 3, \tag{1}$$

where $\boldsymbol{F}$ is the deformation gradient. In Wechsler-Lieberman-Read (WLR) theory,[25] $\boldsymbol{F}$ is the distortion matrix which is the measure of the crystal deformation.

To design a micropump, pressure is usually applied from either above or below depending on the actuation method. It includes the evacuation and pressurization types.[16] Suppose a hydrostatic pressure $p^{(h)}$ is applied on the lower surface of the film. The total energy of such a film per unit film thickness is

$$\begin{aligned} e_1^{(h)}[\boldsymbol{y}] = \frac{1}{h}\int_{S\times(0,h)} \Big\{ &\kappa^2 |\nabla^2 \boldsymbol{y}|^2 \\ &+ \varphi\left(\nabla \boldsymbol{y},\ \frac{x_1}{d},\ \frac{x_2}{d},\ \frac{x_3}{h}\right)\Big\} dx_1 dx_2 dx_3 \\ &- \frac{P}{3}\int_{S\times\{0\}} \boldsymbol{y}\cdot\left(\frac{\partial \boldsymbol{y}}{\partial x_1}\times\frac{\partial \boldsymbol{y}}{\partial x_2}\right) dx_1 dx_2, \end{aligned} \tag{2}$$

where $P = \frac{p^{(h)}}{h}$ is assumed to be a constant. Above $\frac{\partial \boldsymbol{y}}{\partial x_i} = \left(\frac{\partial y_1}{\partial x_i},\ \frac{\partial y_2}{\partial x_i},\ \frac{\partial y_3}{\partial x_i}\right)$, $\nabla \boldsymbol{y} = \left(\frac{\partial y_i}{\partial x_j}\right)$, $\nabla^2 \boldsymbol{y} = \left(\frac{\partial^2 y_i}{\partial x_j \partial x_k}\right)$ for $i,\ j,\ k = 1,\ 2,\ 3$, and

$$|\nabla^2 \boldsymbol{y}|^2 = \sum_{i=1}^{3}\sum_{j=1}^{3}\sum_{k=1}^{3}\left|\frac{\partial^2 y_i}{\partial x_j \partial x_k}\right|^2.$$

Further, $\boldsymbol{a}\cdot\boldsymbol{b}$ and $\boldsymbol{a}\times\boldsymbol{b}$ are the standard notations for the inner and cross products of two vectors $\boldsymbol{a}$ and $\boldsymbol{b}$. The term

$$\frac{1}{3}\int_{S\times\{0\}} \boldsymbol{y}\cdot\left(\frac{\partial \boldsymbol{y}}{\partial x_1}\times\frac{\partial \boldsymbol{y}}{\partial x_2}\right) dx_1 dx_2$$

is the volume enclosed between the plane $\boldsymbol{y}_{\boldsymbol{A}}(S\times\{0\})$ and the deformed lower surface of the film $\boldsymbol{y}(S\times\{0\})$ where $\boldsymbol{y}_{\boldsymbol{A}}(\boldsymbol{x}) := \boldsymbol{A}\boldsymbol{x}$ and $\boldsymbol{A}$ is a constant 3×3 matrix (see Ref. 12)) for the detailed discussion). Note that if the film is not stretched as deposited, $\boldsymbol{A} = \boldsymbol{I}$ where $\boldsymbol{I}$ is the identity matrix.

The interpretation of eq. (2) is as follows. The first term is the van der Waals type of interfacial energy which penalizes changes in the deformation gradient. Minimizers of the energy eq. (2) have oscillations on a length scale that scale with κ and hence we call κ the length scale of the microstructure. The second term is the elastic energy with density φ. It depends on deformation gradient $\boldsymbol{F}$ which is the measure of the distortion of the crystal lattice. The dependence of φ on the material point $\boldsymbol{x}$ reflects the fact that the film is not homogeneous. The final term is interpreted as the energy of a fluid under the film with pressure P.

To understand the behavior of this film, we need to minimize its energy eq. (2) amongst all possible deformations $\boldsymbol{y}$ at pressure P. This is a rather difficult problem since φ is not a convex function of deformation gradient $\boldsymbol{F}$. For a shape-memory material φ is nonconvex, with multi-well structure—one well for each phase or variant. This creates serious problems because of the difficulty in nonconvex minimization. Another difficulty arises from *size effects* due to inhomogeneity of the film. We assume that the film is heterogeneous and contains three length scales: the film thickness h, the typical grain size d and the microstructure length scale governed by κ. The properties of the film are crucially determined by the different ratios of these three length scales. Fortunately, we know that the lateral extent (*i.e.*, the in-plane dimensions) of the film is much larger than any of the length scales κ, d or h. The macroscopic behavior of the film does not depend on every detail of the grains and multilayers, but only on some average features. Thus, one can find an *effective theory* for this heterogeneous film in the limit when all length scales tend to zero, but with possibly different limiting ratios. Shu[21] has used the framework of Γ-convergence to show that the average behavior of the film is determined by an effective two-dimensional theory. The limiting theory implies that the overall deformation $\boldsymbol{y}$ has three components y_1, y_2 and y_3 which depend only on the in-plane variable x_1 and x_2. In addition, the deformation $\boldsymbol{y}$ of the film is determined by minimizing the *effective potential energy*

$$e_1^0[\boldsymbol{y}] = \int_S \left\{ \bar{\varphi}\left(\frac{\partial \boldsymbol{y}}{\partial x_1}, \frac{\partial \boldsymbol{y}}{\partial x_2}\right) - \frac{P}{3}\boldsymbol{y}\cdot\left(\frac{\partial \boldsymbol{y}}{\partial x_1} \times \frac{\partial \boldsymbol{y}}{\partial x_2}\right)\right\} dx_1 dx_2, \tag{3}$$

where $\bar{\varphi}$ is the *effective, macroscopic* or *overall* energy density of the heterogeneous film.[12,22] Note that the density $\bar{\varphi}$ depends only on the in-plane deformation gradient $\bar{\boldsymbol{F}}$ which is a 3×2 distortion matrix

$$\bar{F}_{i\alpha}(x_1, x_2) = \frac{\partial y_i(x_1, x_2)}{\partial x_\alpha}, \quad \text{for} \quad i = 1, 2, 3 \quad \text{and} \quad \alpha = 1, 2. \tag{4}$$

The interpretation and determination of $\bar{\varphi}$ for various conditions are given in Sec. 3 and Sec. 4.

3. Recoverable Deformation and Energy Minimization

3.1 Recoverable deformation

Consider a shape-memory alloy on the high temperature austenite phase and choose this as the reference configuration. As it is cooled, it transforms to martensite with cubic lattice structure changed to less symmetric structure such as tetragonal, trigonal, orthorhombic or monoclinic symmetry. This gives rise to k symmetry-related variants of martensite. Each variant has its own transformation or Bain matrix $\boldsymbol{U}_i$, which describes the distortion of the lattice. For example, an alloy of Cu–Zn–Al undergoes a cubic to monoclinic-II transformation. The number of martensitic variants is 12 (so $k = 12$ in this case) for such an alloy and one of the distortion matrices is

$$\boldsymbol{U}_1 = \begin{pmatrix} p & q & 0 \\ q & r & 0 \\ 0 & 0 & s \end{pmatrix}, \tag{5}$$

where $p = 1.089$, $q = 0.025$, $r = 1.007$ and $s = 0.9093$ for Cu–17 at%Zn–15 at%Al.[7] Other transformation matrices $\boldsymbol{U}_2, \cdots, \boldsymbol{U}_{12}$ can be determined from $\boldsymbol{U}_1$ by symmetry: $\boldsymbol{U}_i = \boldsymbol{R}_i \boldsymbol{U}_1 \boldsymbol{R}_i^T$ where $\boldsymbol{R}_i$ is an orthogonal matrix in the point group of austenite. Since deformation associated with these distortion matrices are stress-free, the elastic density φ has the lowest energy states at these well points $\boldsymbol{U}_i$ for $i = 1, \cdots, k$. We may therefore assume that the density $\varphi(\boldsymbol{F})$ is nonnegative, and is zero at well points $\boldsymbol{U}_i$. Note that if $\boldsymbol{Q}$ is a proper rotation matrix, then $\varphi(\boldsymbol{Q}\boldsymbol{U}_i) = 0$ by frame-indifference.

When a bulk shape-memory alloy is cooled below the critical temperature, it can from microstructures by coherently mixing the variants of martensite to accommodate deformation. When it is subsequently heated, each variant goes back to the austenite and all the deformation is recovered. Thus, $\boldsymbol{F}$ is recoverable if the material can accommodate it by making some microstructure of martensite. It turns out that recoverable deformations are not restricted only to those wells points $\boldsymbol{Q}\boldsymbol{U}_i$ where $\boldsymbol{Q}$ is any proper rotation; instead, they include all possible combination of these wells as long as the fine-scale mixtures of variants are coherent. Thus, the behavior of a shape-memory alloy is governed not by the microscopic energy density φ, but the *effective density* $\bar{\varphi}$ determined by energy minimization. In our energetic point of view, energy minimization with multi-well density φ leads to minimizing sequences which we interpret as microstructure or fine-scale mixtures of variants. Physically, $\bar{\varphi}(\boldsymbol{F})$ is the average stored energy density of the alloy when the average deformation gradient is $\boldsymbol{F}$ after taking into account the martensitic microstructure. Finally, the effective density $\bar{\varphi}$ has a very important property that it vanishes on the set $\mathscr{P}_b$

$$\mathscr{P}_b = \{\boldsymbol{F} \in M^{3\times3} : \bar{\varphi}(\boldsymbol{F}) = 0\} \quad \text{(Bulk Materials)}, \tag{6}$$

where $M^{3\times3}$ is the set of all 3×3 matrices. Any $\boldsymbol{F} \in \mathscr{P}_b$ is recoverable since material can accommodate it by making a mixture of martensitic variants and $\varphi(\boldsymbol{Q}\boldsymbol{U}_i) = 0$ for each variant $\boldsymbol{U}_i$ and for any proper rotation $\boldsymbol{Q}$.

Returning to thin films. We use the same notation $\bar{\varphi}$ for the effective density of the film. It determines the overall behavior of the film. From the limiting theory eq. (3), $\bar{\varphi} = \bar{\varphi}(\bar{\boldsymbol{F}})$ where $\bar{\boldsymbol{F}}$ is a 3×2 distortion matrix eq. (4). Therefore, the set of recoverable deformation is not eq. (6), but replaced by

$$\mathscr{P}_f = \{\bar{\boldsymbol{F}} \in M^{3\times2} : \bar{\varphi}(\bar{\boldsymbol{F}}) = 0 \quad \text{(Thin Films)} \tag{7}$$

for the film. Above note that $M^{3\times2}$ is the set of all 3×2 matrices.

3.2 Taylor bound

We wish to determine which deformation is recoverable on heating. This is equivalent to finding the sets $\mathscr{P}_b$ for bulk materials and $\mathscr{P}_f$ for thin films. However, it is in general a very difficult problem. The determination of the sets $\mathscr{P}_b$ or $\mathscr{P}_f$ is largely an open problem in literature. We do not know these two sets, except in some very special cases. Saburi and Nenno[20] have given a qualitative but very insightful discussion on recoverable deformation. Bhattacharya[1] has used the framework of geometrically linear theory to determine recoverable linear strains for most martensitic single crystals.

The problem becomes even harder for polycrystals. A polycrystal is made up of a number of subregions called grains. Each grain is made up of identical crystals with different orientations. So $\boldsymbol{F}_0$ is recoverable if there exists a compatible field $\boldsymbol{F}(\boldsymbol{x})$ with average equal to $\boldsymbol{F}_0$ and is recoverable for each grain. However, the grains are constrained one another by their neighbors. Thus, this field can be quite complicated and therefore it is very difficult to calculate the set $\mathscr{P}_b$. Bhattacharya & Kohn[4,5] and Shu & Bhattacharys[23] have used the framework of geometrically linear theory and the Taylor bound to estimate recoverable strain in a general polycrystal. The idea of Taylor bound is that each grain is assumed to undergo identical deformation to avoid intergranular incoherence. Further, the overall deformation is recoverable if it is recoverable for every grain of the polycrystal. Shu and Bhattacharya[23] have demonstrated that the results obtained from the Taylor bound are surprisingly good in estimating recoverable strain and agree very well with experiment. Bhattacharya and Kohn[5] have derived rigorous results to support this argument. So from now on, we will use the

Taylor bound as our fundamental tool for evaluating the effect of texture.

4. Effective Behavior

4.1 Single crystal film

We consider a single crystal film first. Suppose the film is homogeneous; *i.e.*, the bulk density depends only on deformation gradient: $\varphi = \varphi(\boldsymbol{F})$. In this case, the effective or relaxed density of the film can be shown to be[8)]

$$\bar{\varphi}(\bar{\boldsymbol{F}}) = Q\varphi_0(\bar{\boldsymbol{F}}), \quad \varphi_0(\bar{\boldsymbol{F}}) = \min_{\boldsymbol{b}} \varphi(\bar{\boldsymbol{F}}|\boldsymbol{b}), \tag{8}$$

where $\bar{\boldsymbol{F}}$ is the 3×2 distortion matrix defined by eq. (4) and $Q\varphi_0$ is the relaxation of density φ_0. The notation $\boldsymbol{F} = (\bar{\boldsymbol{F}}|\boldsymbol{b})$ means that the first two columns and final column of the 3×3 matrix $\boldsymbol{F}$ are replaced by $\bar{\boldsymbol{F}}$ and $\boldsymbol{b}$, respectively. The exact definition of $Q\varphi_0$ can be found in[6,8)] and is not shown here as it requires advanced mathematical analysis which is beyond the purpose of this paper.

The major difference between bulk materials and thin films is that the relaxation process is associated with the density φ_0 given by eq. (8) for films. The deformation of the film is determined by two vector fields $\boldsymbol{y}(x_1, x_2)$ and $\boldsymbol{b}(x_1, x_2)$ which depend only on the in-plane variables x_1 and x_2. The vector field $\boldsymbol{y}$ determines the deformation of a middle surface while the vector field $\boldsymbol{b}$ describes the transverse shear and normal compression. Since the last column of the 3×3 distortion matrix $\boldsymbol{F}$ is relaxed by $\boldsymbol{b}$, the out-of-plane compatibility becomes insignificant. The requirement of coherence is therefore weakened in thin films than in bulk materials. This allows a variety of deformation such as "paper-folding" deformations, "tunnels" and "tents" in single crystal films.[3)]

We wish to determine the set of recoverable deformation defined by eq. (7) for single crystal films with density $\bar{\varphi}$ given by eq. (8). However, it is not an easy task and the determination of this set can be found only in some special cases.[2)] We then look for the following approximation. The frame-indifference implies that the energy density φ_0 has to satisfy $\varphi_0(\bar{\boldsymbol{F}}) = \varphi_0(\boldsymbol{Q}\bar{\boldsymbol{F}})$ for all possible 3×2 distortion matrices $\bar{\boldsymbol{F}}$ and for all 3×3 proper rotations $\boldsymbol{Q}$. This also implies that there exists a function W such that $\varphi_0(\bar{\boldsymbol{F}}) = W(\sqrt{\bar{\boldsymbol{C}}})$ where $\bar{\boldsymbol{C}} = \bar{\boldsymbol{F}}^T\bar{\boldsymbol{F}}$ is a 2×2 positive semi-definite symmetric matrix.[8)] It follows that the effective density $\bar{\varphi}$ also depends only on $\bar{\boldsymbol{C}}$ or $\bar{\varphi}(\bar{\boldsymbol{F}}) = \bar{W}(\sqrt{\bar{\boldsymbol{C}}})$ for some function $\bar{W}$.

Let u_1, u_2 and η be the in-plane displacement and out-of-plane deflection of the film. They are defined by $u_1 = y_1 - x_1$, $u_2 = y_2 - x_2$, $y_3 = \eta$. For pressurized shape-memory films, the out-of-plane deflection η is expected to be much larger than the film thickness: $\eta \gg h$. Further, the film is constrained on the boundary. We then assume $|u_{1,\alpha}u_{1,\beta}| \ll 1$, $|u_{2,\alpha}u_{2,\beta}| \ll 1$ for $\alpha, \beta = 1, 2$, but retain the nonlinear contribution coming from gradients of deflection. It follows that the finite strain measure $\sqrt{\bar{\boldsymbol{C}}}$ can be approximated to

$$\sqrt{\bar{\boldsymbol{C}}} - I \approx \bar{\boldsymbol{E}} = \bar{\boldsymbol{E}}[\boldsymbol{u}, \eta] = \boldsymbol{\varepsilon}^1[\boldsymbol{u}] + \boldsymbol{\varepsilon}^2[\eta],$$

$$\varepsilon^1_{\alpha\beta}[\boldsymbol{u}] = \frac{1}{2}\left(\frac{\partial u_\alpha}{\partial x_\beta} + \frac{\partial u_\beta}{\partial x_\alpha}\right),$$

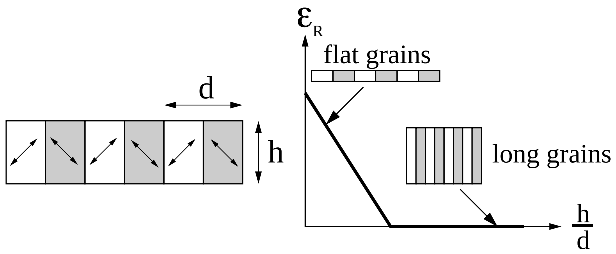

Fig. 2 The recoverable extension ε_R versus aspect ratio $\frac{h}{d}$ of the film thickness to grain size. The polycrystalline film has a periodic texture containing two orientations: "grey" and "white" columnar grains.

$$\varepsilon^2_{\alpha\beta}[\eta] = \frac{1}{2}\frac{\partial\eta}{\partial x_\alpha}\frac{\partial\eta}{\partial x_\beta} \tag{9}$$

for $\alpha, \beta = 1, 2$. The microscopic energy density of the film is then approximated to $\varphi_0(\bar{\boldsymbol{F}}) = W(\sqrt{\bar{\boldsymbol{C}}}) \approx W(\bar{\boldsymbol{E}})$ which satisfies

$$W(\bar{\boldsymbol{E}}) \begin{cases} = 0 & \bar{\boldsymbol{E}} \in \bar{\boldsymbol{E}}^{(1)} \cup \bar{\boldsymbol{E}}^{(2)} \cup \cdots \cup \bar{\boldsymbol{E}}^{(k)}, \\ > 0 & \text{otherwise}, \end{cases} \tag{10}$$

where

$$\bar{\boldsymbol{E}}^{(i)} = \sqrt{\bar{\boldsymbol{U}}_i^T\bar{\boldsymbol{U}}_i} - \boldsymbol{I}_p, \quad i = 1, \cdots, k, \tag{11}$$

$\boldsymbol{I}_p$ is the 2×2 identity matrix, and $\bar{\boldsymbol{U}}_i$ is a 3×2 matrix obtained by deleting the last columnar of the 3×3 distortion matrix $\boldsymbol{U}_i$ such as that given by eq. (5).

Our task is to determine recoverable strains using approximate kinematics given by eq. (9). Recalling eq. (7), we see that it is equivalent to finding the set

$$\mathcal{S}_f = \{\bar{\boldsymbol{E}} : \bar{W}(\bar{\boldsymbol{E}}) = 0\}, \tag{12}$$

where the effective density $\bar{\varphi}(\bar{\boldsymbol{F}})$ is approximated by $\bar{W}(\bar{\boldsymbol{E}})$ for certain function $\bar{W}$. Note that we have used the symbol $\mathcal{S}_f$ in eq. (12) instead of $\mathcal{P}_f$ given by eq. (7) to emphasize that the film considered here is a single crystal. If the out-of-plane deflection η is neglected and only the in-plane displacements u_1 and u_2 are considered, this set $\mathcal{S}_f$ can be determined for most shape-memory films undergoing cubic to tetragonal, trigonal and orthorhombic transformations as well as certain oriented Ti–Ni and Cu-based films.[3)] However, the problem becomes hard if the out-of-plane deflection is retained such as the case in pressurized films. In that situation, the determination of the set $\mathcal{S}_f$ is complicated and we refer to[22)] for detailed analysis.

4.2 Heterogeneous Films

4.2.1 Columnar films

Shape-memory thin films are usually made by sputtering.[9,11,14,18,24)] The grains in these films are typically columnar (*e.g.*, see Fig. 2 of Ref. 11)). Further, the microstructure is usually smaller than the grains (*e.g.*, see Fig. 5 in Ref. 13)). So we may assume that the elastic density $\varphi = \varphi(\nabla\boldsymbol{y}, x_1, x_2)$ in eqs. (1) and (2) and $d \gg \kappa$. We can show that the elastic energy dominates the interfacial energy and materials can form microstructures freely. As a result, the macroscopic energy density $\bar{\varphi}$ is *impervious to the presence of interfacial energy*. We can further show that the behavior of the film depends on the ratio of the film thickness h to the typical size of grains d. Table 1 contrasts the behavior of films with long or rod-

Table 1 The predicted uniaxial recoverable extension for various textures in Ti–Ni and Cu-based thin films.

Texture	Uniaxial recoverable strains (%)			
	Ti–Ni		Cu–Zn–Al	
	Long grains	Flat grains	Long grains	Flat grains
Random	2.3	2.3	1.7	1.7
{111} film	5.3	8.1	1.9	5.9
{100} film	2.3	2.3	7.1	7.1
{110} film	2.3	2.3	1.7	1.7

like ($h \gg d$) grains and films with flat or pan-cake shaped ($h \ll d$) grains. It lists the predicted recoverable extension for films with different textures in Ti–Ni and Cu–Zn–Al. Note that they are larger for flat grains compared to long grains. We also note here that neither the random nor {110} texture which is common for BCC materials[9,24] are ideal textures for large recoverable extension. The ideal textures appear to be {100} for Cu–Zn–Al (this texture can be produced by melt-spinning) and {111} for Ti–Ni. We now briefly explain the ideas behind these results.

1. **Flat columnar grains**
   Consider a columnar film with flat grains ($d \gg h$). The grains are flat and thin and have "pan-cake" shape. The intergranular constraints are now only in-plane and this allows a wider class of microstructures formed in thin films than in bulk materials. Any out-of-plane incompatibility is easily overcome with very small elastic energy. Further, within each grain the interface condition is an "invariant line" rather than an "invariant plane" condition. Therefore, the effective behavior of the film is obtained by passing to the two-dimensional limit first and then homogenizing in the plane of the film. Specifically, let $\bar{\boldsymbol{E}}$ be the 2×2 strain matrix obtained by approximating the nonlinear strain measure in eq. (9) and φ_0 be the energy density of each grain with variants given by

$$\varphi_0(\bar{\boldsymbol{E}},\ x_1,\ x_2) \begin{cases} = 0 & \bar{\boldsymbol{E}} \in \bar{\boldsymbol{E}}^{(1)} \cup \bar{\boldsymbol{E}}^{(2)} \cup \cdots \bar{\boldsymbol{E}}^{(k)}, \\ > 0 & \text{otherwise}, \end{cases} \tag{13}$$

   where

$$\bar{\boldsymbol{E}}^{(i)} = \Pi \boldsymbol{R} \boldsymbol{E}^{(i)} \boldsymbol{R}^T \Pi^T,$$

$$\boldsymbol{E}^{(i)} = \sqrt{\boldsymbol{U}_i^T \boldsymbol{U}_i} - \boldsymbol{I}, \quad \Pi = \begin{pmatrix} 1 & 0 & 0 \\ 0 & 1 & 0 \end{pmatrix}, \tag{14}$$

   where $\boldsymbol{U}_i$ is the 3×3 distortion matrix such as that in eq. (5), $\boldsymbol{I}$ is the 3×3 identity, and $\boldsymbol{R} = \boldsymbol{R}(x_1,\ x_2)$ is the rotation matrix describing the orientation of the grains. The effective density $\bar{\varphi} = \bar{W}(\bar{\boldsymbol{E}})$ of the polycrystalline film is then obtained by homogenizing the inhomogeneity x_1, x_2 in eq. (13). The overall strain $\bar{\boldsymbol{E}}$ is recoverable if $\bar{W}(\bar{\boldsymbol{E}}) = 0$. We use the Taylor bound described in Sec. 3.2 to estimate recoverable extension for various cases and the results are listed in Table 1.

2. **Long columnar grains**
   We now turn to another extreme case $h \gg d$. The grains are now long and rod-like; and it is no longer possible to overcome out-of-plane constraints. Therefore, the intergranular constraints are fully three-dimensional. Consequently, the effective behavior is obtained by homogenizing in three dimensions and then passing to the two-dimensional limit. As a result, the estimation of recoverable strains for such films is basically similar to bulk materials. Table 1 lists predicted recoverable extension for Ti–Ni and Cu–Zn–Al films with various textures. Recoverable extension is smaller than that for the same films but with flat grains since the intergranular constraints are weakened in films with flat grains.

3. **Comparable grains**
   While these extreme cases are instructive, the film thickness and the grain size are on the same order of magnitude in sputtered films. The analysis is then difficult but reflects the trends suggested by the extreme cases. Let us use the following example to demonstrate it. Consider a two-dimensional polycrystalline film with a texture containing two orientations ("grey" and "white" grains) as shown in Fig. 2. Assuming that the martensite has two variants, we can calculate the recoverable extension exactly for any value of the ratio $\frac{h}{d}$. The result is shown schematically in Fig. 2. The dependence is striking, and the recoverable strain is maximum at $\frac{h}{d} = 0$ (flat grains) and minimum at $\frac{h}{d} = \infty$ (long grains) as expected.

4.2.2 Extremely small grains

We now consider the effect of the ratio $\frac{\kappa}{d}$ of the size of the microstructure to that of the grain. Above, we took this ratio to be zero; however, this may not be true when the grain size becomes very small (on the order of tens of nanometer). We can show that if $\kappa \gg d$, it costs materials more energy to form microstructure inside each grain and consequently strains can not be recovered unless the texture is exceptional. Our result[21] shows that the effective behavior of the film is obtained by averaging the properties of small grains, then passing to the two-dimensional limit. Finally, the analysis on the case of comparable κ and d is difficult but it interpolates the two extreme cases.

4.2.3 Multilayers

Consider a multilayered film made up of a finite number of alternating layers of a martensitic material and a purely elastic material. Let λ be the volume fraction of the martensitic material and ε_I be the strain due to some internal stress of the elastic material relative to the austenite phase of the martensitic material. The effective behavior is some combination of the behavior of these two materials; however, the nature of the behavior depends on the ratio $\frac{\kappa}{h}$ of the microstructure size to the thickness. We demonstrate with an example assuming a two-variant martensite with transformation strains $-\varepsilon_M$ and ε_M for simplicity. At high temperature, the multilayer consists of alternating layers of two elastic materials. The overall strain of this multilayer is ε_0 which is pretty close to zero since the austenite has a strong modulus. At low temperature, Fig. 3 contrasts the behavior of multilayers with small $\frac{\kappa}{h}$ and multilayers with large $\frac{\kappa}{h}$. The thin continuous line is the energy of the martensitic material and the thin dashed line is the energy of the elastic material. The behavior of the multilayer is shown by thick continuous line. For small $\frac{\kappa}{h}$, the martensitic material freely forms microstructure and the multilayer is like

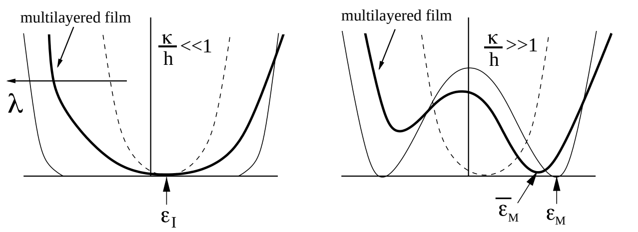

Fig. 3 The effective behavior of a multilayered film is determined by the energies above for small and large values of $\frac{\kappa}{h}$ of the microstructure size to the thickness. Note that ε_0 is not shown above and $0 < \varepsilon_0 < \varepsilon_I$ since the austenite has null transformation strain.

an elastic material with soft modulus. Further, the internal strain ε_I is completely accommodated by forming martensitic microstructure at low temperature. As a result, this layered film will show a two-way shape-memory effect by cycling temperature to obtain strain ε_0 (high temperature) and strain ε_I (low temperature). But the effect is weak as the difference between ε_0 and ε_I is small and the overall modulus of the multilayer is soft at low temperature.

For large $\frac{\kappa}{h}$ on the other hand, the multilayer behaves like a phase transforming material: it has two variants with transformation strains which may be different from that of the original martensitic material, and one variant is preferred over the other. The preferred variant of the multilayer has an overall strain $\bar{\varepsilon}_M$ which is close to ε_M. Hence, this multilayered film will display a strong two-way shape-memory effect: cycling temperature leads to strain to cycle between ε_0 and $\bar{\varepsilon}_M$ as shown in Fig. 3. Note that the difference between ε_0 and $\bar{\varepsilon}_M$ is large since the martensite has large transformation strain and $\varepsilon_M \approx \bar{\varepsilon}_M$. Further notice that the multilayer is internally stressed so that the minimum energy is not zero. Finally, the multilayer can form "macroscopic twins": these are not twins confined to the martensitic material but encompass both the elastic and the martensitic material. Thus, multilayers promise to be a means of making apparently new materials.

5. Application to Micropumps

We now apply our theory to the design of shape-memory micropumps with pumping volume as much large as possible. Consider a film deposited on the substrate in the austenite state. Assume that the film is unstressed as deposited and is constrained to the boundary so that the in-plane displacements u_1, u_2 and out-of plane deflection η are zero on the boundary. Minimizing the effective energy eq. (3) with respect to all possible recoverable deformations gives

$$\min e_1^{(0)}[u_1,\ u_2,\ \eta] = -P \max \int_S \eta(x_1,\ x_2) dx_1 dx_2, \qquad (15)$$

where the minimization is taken over all possible recoverable deformations such that eq. (7) holds. The right-hand-side of eq. (15) is the change of the volume of the film subjected to constant pressure P. To maximize this term, we may resort to maximizing the deflection η over all possible recoverable deformation. Therefore, we use the ratio m of the central deflection to the half-edge length of the diaphragm as a criterion of ability to recover large strain.

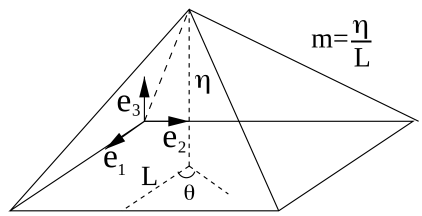

Fig. 4 A square tent.

5.1 Single crystal micropumps

Consider a pressurized film made of a shape-memory single crystal. The exact effective density is in general unavailable due to various causes, and this makes it difficult to determine recoverable deflection for this film. Fortunately, we can use eq. (15) to estimate it with needed information only for well points or variants given by eq. (10).

Consider a square diaphragm and assume that the deformed shape is a tent as shown in Fig. 4. Let m be the ratio of the central deflection of the film to the half-edge length of the square domain. We use simplified kinematics $\bar{\boldsymbol{E}}$ defined by eq. (9) to approximate the finite strain measure. Further, to satisfy the fixed end boundary condition, we assume the "macroscopic" in-plane displacement $\boldsymbol{u}(x_1,\ x_2) = 0$ for $(x_1,\ x_2) \in S$. The gradients of the deflection η of the tent are

$$\begin{pmatrix} \dfrac{\partial \eta}{\partial x_1} \\ \dfrac{\partial \eta}{\partial x_2} \end{pmatrix} = \begin{pmatrix} m \\ 0 \end{pmatrix}, \begin{pmatrix} 0 \\ -m \end{pmatrix}, \begin{pmatrix} -m \\ 0 \end{pmatrix}, \begin{pmatrix} 0 \\ -m \end{pmatrix}. \qquad (16)$$

Using eqs. (9), eq. (12) and (16) gives the condition for stress-free strain

$$\bar{\boldsymbol{E}} = \begin{pmatrix} \frac{1}{2}m^2 & 0 \\ 0 & 0 \end{pmatrix}, \begin{pmatrix} 0 & 0 \\ 0 & \frac{1}{2}m^2 \end{pmatrix} \in \mathcal{S}_f, \qquad (17)$$

where $\mathcal{S}_f$ given by eq. (12) is the set of all recoverable strains for the single crystal film.

Consider a 4-well problem which arises in the cubic to monoclinic-II transformation. Let the transformation strains be

$$\bar{\boldsymbol{E}}^{(1)} = \begin{pmatrix} \alpha & \delta \\ \delta & \gamma \end{pmatrix}, \quad \bar{\boldsymbol{E}}^{(2)} = \begin{pmatrix} \alpha & -\delta \\ -\delta & \gamma \end{pmatrix},$$

$$\bar{\boldsymbol{E}}^{(3)} = \begin{pmatrix} \gamma & \delta \\ \delta & \alpha \end{pmatrix}, \quad \bar{\boldsymbol{E}}^{(4)} = \begin{pmatrix} \gamma & -\delta \\ -\delta & \alpha \end{pmatrix},$$

where $\alpha > 0$, $\gamma > 0$, $\delta > 0$. In this case, it can be shown that the recoverable set $\mathcal{S}_f$ contains the convex combination of $\bar{\boldsymbol{E}}^{(1)}, \cdots, \bar{\boldsymbol{E}}^{(4)}$.[22] However, one can show that eq. (17) can not be satisfied unless the crystal basis is rotated with some angle θ with respect to the film basis $\boldsymbol{e}_3$. Indeed, choosing $\cos 2\theta = \frac{\alpha-\gamma}{\alpha+\gamma}$, we obtain

$$m = \sqrt{2(\alpha + \gamma)}. \qquad (18)$$

For Cu–Zn–Al, $\alpha = 0.089$, $\delta = 0.025$, $\gamma = 0.007$, we have $m = 0.438$ and $\theta = 15.7°$. Note that Hane[10] has used the fully finite deformation kinematics and Bhattacharya-James

Table 2 The predicted ratio of the maximum recoverable deflection to the radius of the circular diaphragm for various films with different textures. Ni–Al, Cu–Al–Ni, Ti–Ni and Cu–Zn–Al alloys undergo cubic to tetragonal, to orthorhombic, to monoclinic-I and to monoclinic-II transformations, respectively.

Texture	m: maximum deflection/radius			
	Ni–Al	Cu–Al–Ni	Ti–Ni	Cu–Zn–Al
{100} film	0.18	0.19	0.15	0.20
{111} film	—	0.08	0.13	0.09
{110} sputtered film	—	0.10	0.15	0.09

thin film theory[3] to obtain $m = 0.45$ and $\theta = 15.6°$.

5.2 Polycrystalline micropumps

We turn to practical cases—polycrystalline thin films with common {100}, {110} or {111} textures. In this situation, the properties of the film are basically transversely isotropic. So we consider a circular diaphragm and set m be the ratio of the maximum central deflection to the radius of the circular domain. We assume that the grains are columnar and the grain sizes are much larger than the film thickness ($d \gg h$). The result of Sec. 4.2.1 suggests that the effective energy density of films is obtained by first passing to the two-dimensional limit and then homogenizing in-plane heterogeneity. Unfortunately, the exact form of effective density is not easy to be found for a general polycrystalline film. Therefore, we have to resort to the Taylor bound described in Sec. 3.2 for estimating recoverable deflection. We can show that[22]

$$m = \frac{\eta_0}{r_0} \propto \max_i \sqrt{\bar{E}_{11}^{(i)} + \bar{E}_{22}^{(i)} - \varepsilon_I} \tag{19}$$

where η_0 and r_0 are the central deflection and radius of the diaphragm, $\bar{\boldsymbol{E}}^{(i)}$ is ith transformation strain given by eq. (14), ε_I is the internal or misfit tensile strain exerted from the remaining part of the film adhered to the substrate. Above in eq. (19) the maximum is over all possible variants.

Table 2 shows the ratio m for a variety of shape-memory films with certain common textures. We assumed $\varepsilon_I = 0$ in our calculation. We see that the ratio m for {110} sputtered Ti–Ni film is about 0.15, and is almost the same for other textured Ti–Ni films. So recoverable deflection is insensitive to texture for Ti–Ni film. It is surprising to see relatively small recoverable deflection for {111} Ti–Ni films which are able to recover large uniaxial tensile strain as seen from Table 1. This is due to the fact that the diaphragm is sustained to biaxial tensile strain simultaneously instead of one-dimensional extension. Next we find that the ratio m is large for {100} Cu-based shape-memory film and is sensitive to texture for other Cu-based films. It follows that {100} Cu-based film can have better behavior than Ti–Ni film in view of large recoverable deflection. Finally, we may apply our result to the design of pizeoelectricly actuated micropumps. For example, $PbTiO_3$ is a ferroelectric material with crystal structure undergoing cubic to tetragonal transformation. It can be shown that $m = 0.1$ for {100} $PbTiO_3$ textured film.

Table 3 The comparison of the prediction with several experimental observations for Ti–Ni films.

	Prediction	Wolf & Heuer[26]	Miyazaki *et al.*[17]	Makino *et al.*[16]
$m = \dfrac{\text{deflection}}{\text{radius}}$	0.15	0.12	0.07	0.04

6. Comparison with Experiment

Wolf and Heuer[26] have deposited a Ti–Ni film on a silicon substrate by RF sputtering. They have used microfabrication technique to create Ti–Ni square diaphragms, which exhibited fair shape-memory behavior and other desired mechanical properties. They have reported that the work density of Ti–Ni diaphragm is at least 5×10^6 J/m^3, which is higher than any other type of microactuation. The ratio of maximum recoverable deflection to the half-edge length of the square diaphragm is about 0.12 as shown in Table 3. Our predicted value is slightly higher than their experimental observation and there are various reasons for it. First, the maximum recoverable deflection defined here refers to stress-free deformation which maximizes the change of volume of the diaphragm eq. (15). Ideally, the maximum ratio m is independent of the magnitude of the applied pressure. However, in reality, a suitable magnitude of pressure is needed to initiate the movement of martensitic variants to achieve large deflection. Wolf and Heuer[26] have claimed to expect larger recoverable deflection by increasing pressure while they did not perform it due to the limitation of the experimental facility. Second, we assume that the film has a perfect {110} texture with grain size much larger than the film thickness ($d \gg h$). We are not clear whether this assumption holds or not for their experiment. Finally, there is a shape anisotropy since the predicted value is obtained for a circular diaphragm while the diaphragm used in experiment is a square.

Miyazaki *et al.*[17,19] have deposited a Ti–Ni film on a Si substrate with SiO_2 surface by RF magnetron sputtering method. A diaphragm has been fabricated by applying Si photoetching, leaving a free standing multilayer with Ti–Ni on the top and SiO_2 on the bottom. They have cleverly created a two-way shape-memory diaphragm by taking advantage of different thermal expansion coefficients among Ti–Ni, SiO_2 and Si. The reference state has been set up in the high temperature phase. As a result, the in-plane dimension of SiO_2 is relative wider than that of Si at low temperature, causing the buckle of SiO_2 layer. The buckle is upward since the in-plane dimension of Ti–Ni is smaller than that of SiO_2 at low temperature. The ratio of the central deflection to the half-edge length of the diaphragm has been measured to be around 0.07 which is smaller than what we predict theoretically. The difference is explained as follows. Their idea to develop a two-way shape-memory effect is somewhat similar to that using multilayers consisting of alternating layers of elastic and martensitic materials as explained in Sec. 4.2.3. The change of the shape of multilayer described in Sec. 4.2.3 is primarily due to membrane stretching while the shape change in the experiment of[17] is due to the combination of stretching and bending at low temperature. The stretching can be relieved by forming martensitic microstructure while the bending resulting from some internal stress provides a less significant role to produce large deflection. Further, if the ratio $\frac{\kappa}{h}$ of the microstructure size to the thickness is small in experiment,[17] the two-way shape-memory effect obtained by cycling thermal strain is weak as explained in Sec. 4.2.3.

Finally, Makino *et al*.[15,16] have successfully fabricated a Ti–Ni actuated micropump with pumping pressure up to several hundreds of kPa. The measured ratio of deflection to the half-edge length of the Ti–Ni diaphragm is about 0.04. Clearly, from Table 3, our theoretical prediction is larger than this value. The discrepancy is not completely understood here. The theoretical calculation is based on the {110} sputtering texture while the Ti–Ni film made in experiment is produced by flash evaporation method. So the texture we use in the calculation may not be the one in experiment. Next, we assume that the film is unstressed as deposited in our calculation. However, an internal tensile stress may exist during deposition (for example, see[13,26]). If that happened, the Ti–Ni diaphragm is subject to bi-axial pre-tensile stress resulting from the remaining part of the film adhered to Si substrate. In that case, the central recoverable deflection will decrease significantly due to eq. (19). However, there is no evidence to see the existence of internal stresses in the experiment of Makino *et al*.[15,16]

7. Conclusion

We have investigated the behavior of pressurized shape-memory films with application to the design of large stroke micropumps. We start with a theoretical framework accounting in detail for the underlying microstructure, grain size, film thickness as well as their interactions. We show that the behavior of thin film is different from that of bulk material. We also point out that a heterogeneous film shows strong size effects and its behavior depends crucially on the different ratios of length scales including film thickness, grain size and microstructure length scale. We demonstrate with an example that the recoverable extension is very different for thin films with flat or long columnar grains. We also show that a two-way shape-memory effect can be developed by multilayers made up of alternating layers of a martensitic and a purely elastic material.

We use recoverable deflection as a measure to design large stoke micropumps and develop a model to estimate it. We approximate the finite strain measure using the assumption of von Kármán membrane. We show that the recoverable deflection of a polycrystalline film depends on the transformation strain of the underlying martensitic transformation, the texture and especially on the size effects. Table 2 lists our predictions for recoverable deflection for various shape-memory films with different common textures. We show that the estimation of recoverable deflection is very different from that of recoverable extension since the former is due to bi-axial tensile strain simultaneously while the latter is due to one-dimensional tensile strain. We compare the prediction of maximum recoverable deflection with several experimental observations of Wolf & Heuer,[26] Miyazaki *et al*.[17] and Makino *et al*.[16] The following is a list of our main conclusions and suggestions.

- Flat grains are preferable to long grains in columnar films concerning the purpose of large recoverable deflection and extension.
- Common sputtering {110} texture is not ideal for recoverable deflection and extension in both Ti–Ni and Cu-based shape-memory films.
- Recoverable deflection is not sensitive to common film textures in Ti–Ni films while it is sensitive in Cu-based shape-memory films.
- It turns out that {100} texture is ideal for both recoverable deflection and extension in Cu-based films.
- Multilayered thin films provide a promising avenue for making materials with novel properties.

Acknowledgments

I am grateful to S. Miyazaki and E. Makino for helpful and stimulating discussions. I am glad to acknowledge the partial financial support of the National Science Council of Taiwan under the grant NSC 90-2622-E-002-006.

REFERENCES

1) K. Bhattacharya: Cont. Mech. Thermodyn. **5** (1993) 205–242.
2) K. Bhattacharya and G. Dolzmann: J. Mech. Phys. Solids **48** (2000) 1493–1517.
3) K. Bhattacharya and R. D. James: J. Mech. Phys. Solids **47** (1999) 531–576.
4) K. Bhattacharya and R. V. Kohn: Acta Mater. **44** (1996) 529–542.
5) K. Bhattacharya and R. V. Kohn: Arch. Rat. Mech. Anal. **139** (1997) 99–180.
6) A. Braides and A. Defranceschi: *Homogenization of Multiple Integrals* (Oxford University Press, Oxford, 1998).
7) S. Chakravorty and C. M. Wayman: Acta Metall. **25** (1977) 989–1000.
8) H. Le Dret and A. Raoult: J. Math. Pures. Appl. **74** (1995) 549–578.
9) K. R. C. Gisser, J. D. Busch, A. D. Johnson and A. B. Ellis: Appl. Phys. Lett. **61** (1992) 1632–1634.
10) K. F. Hane: J. Mech. Phys. Solids **47** (1999) 1917–1939.
11) A. Ishida, A. Takei and S. Miyazaki: Thin Solid Films **228** (1993) 210–214.
12) R. D. James and R. Rizzoni: J. Elasticity **59** (2000) 399–436.
13) P. Krulevitch, A. P. Lee, P. B. Ramsey, J. C. Trevino, J. Hamilton and M. A. Northrup: Journal of Microelectromechanical Systems **5** (1996) 270–282.
14) P. Krulevitch, P. B. Ramsey, D. M. Makowiecki, A. P. Lee, M. A. Northrup and G. C. Johnson: Thin Solid Films **274** (1996) 101–105.
15) E. Makino, T. Shibata and K. Kato: Sensors and Actuators A **78** (1999) 163–167.
16) E. Makino, T. Shibata and K. Kato: Sensors and Actuators A **88** (2001) 256–262.
17) S. Miyazaki, M. Hirano and T. Yamamoto: Dynamic Characteristics of Ti–Ni SMA Thin Film Microactuators. Submited to IUTAM, 2001.
18) S. Miyazaki and A. Ishida: Mater. Trans., JIM **35** (1994) 14–19.
19) S. Miyazaki and A. Ishida: Mater. Sci. and Eng. **A273–275** (1999) 106–133.
20) T. Saburi and S. Nenno: In H. I. Aaronson, D. E. Laughlin, R. F. Sekerka and C. M. Wayman, editors, *Proc. Int. Conf. on Solid-Solid Phase Transformations* (The Metall. Soc. AIME, 1981) pp. 1455–1479.
21) Y. C. Shu: Arch. Rational Mech. Anal. **153** (2000) 39–90.
22) Y. C. Shu: In preparation. 2001.
23) Y. C. Shu and K. Bhattacharya: Acta Mater. **46** (1998) 5457–5473.
24) Q. Su, S. Z. Hua and M. Wuttig: J. Alloys and Comp. **211/212** (1994) 460–463.
25) M. Wechsler, D. Liebermann and T. Read: Trans. AIME **197** (1953) 1503–1515.
26) R. H. Wolf and A. H. Heuer: J. Microelectromechanical Systems, **4** (1995) 206–212.